Roder, H., Elove, G., & Englander, S. W. (1988) *Nature (London) 335*, 700–704.
Sargent, D., Benevides, J. M., Yu, M.-H., King, J., & Thomas, G. J., Jr. (1988) *J. Mol. Biol. 199*, 491–502.
Saxena, V. P., & Wetlaufer, D. B. (1970) *Biochemistry 9*, 5015–5022.
Smith, D. H., & King, J. (1981) *J. Mol. Biol. 145*, 653–676.
Snyder, G. H. (1987) *Biochemistry 26*, 688–694.
Stewart, J. M., & Young, J. D. (1984) in *Solid Phase Peptide Synthesis*, 2nd ed., Pierce Chemical Co., Rockford, IL.
Stroup, A. N. (1989) Ph.D. Dissertation, University of Texas Southwestern Medical Center.
Venkatachalam, C. M. (1968) *Biopolymers 6*, 1425–1436.
Villafane, R., & King, J. (1988) *J. Mol. Biol. 204*, 607–619.
Weber, U., & Hartter, P. (1974) *Hoppe-Seyler's Z. Physiol. Chem. 355*, 189–199.
Wright, P. E., Dyson, H. J., & Lerner, R. A. (1988) *Biochemistry 27*, 7167–7175.
Yu, M.-H., & King, J. (1984) *Proc. Natl. Acad. Sci. U.S.A. 81*, 6584–6588.
Yu, M.-H., & King, J. (1988) *J. Biol. Chem. 263*, 1424–1431.
Zhang, R., & Snyder, G. H. (1988) *Biochemistry 27*, 3785–3794.

Articles

Direct and Indirect Pathways of Functional Coupling in Human Hemoglobin Are Revealed by Quantitative Low-Temperature Isoelectric Focusing of Mutant Hybrids†

Vince J. LiCata,‡ Phil C. Speros, Ermanna Rovida,§ and Gary K. Ackers*,‖

Department of Biology, The Johns Hopkins University, Baltimore, Maryland 21218
Received April 16, 1990; Revised Manuscript Received July 16, 1990

ABSTRACT: Functional energetic coupling within human hemoglobin has been explored by using quantitative analysis of asymmetric mutant hybrid equilibria. Previous work showed that the free energy of cooperativity is largely attributable to alterations in free energy that accompany changing interactions at the interface between $\alpha^1\beta^1$ and $\alpha^2\beta^2$ dimers [Pettigrew et al. (1982) *Proc. Natl. Acad. Sci. U.S.A. 79*, 1849]. However, the issue of how cooperativity-linked sites in the molecule are energetically coupled in manifesting cooperative ligation is still not well delineated. In this paper we address the questions of what types of functional coupling pathways are operational in hemoglobin, what some of their characteristics are, and how they are related to one another. By constructing asymmetric mutant hybrid hemoglobins, we can assay how two structurally identical, symmetrically equivalent sites are energetically coupled in manifesting subunit assembly and/or cooperative ligation. Asymmetric hybrid hemoglobins, i.e., those containing a single modified site, cannot be isolated and must be studied in equilibrium with their symmetric parent molecules. In order to study these asymmetric hybrid equilibria, we have developed new theory and quantitation techniques to augment the low-temperature quenching and isoelectric focusing procedures of Perrella et al. [(1978) *Anal. Biochem. 88*, 212]. Studies of these mutant hybrid hemoglobins have provided evidence for three distinct types of energetic coupling within the hemoglobin tetramer. All $\alpha^1\beta^2$ interface sites examined are involved in coooperativity-linked indirect coupling. Within the context of this indirect "pathway" there exist two different types of direct long-range coupling. One of these classes of direct long-range pathways is linked to cooperative ligand binding while the other class is not.

A key issue in structure–function studies of allosteric proteins is how regulatory energy is communicated between relatively distant sites within a molecule or macromolecular assembly. When particular residue sites within a molecule have been identified as being on the pathway for manifesting a particular function, one may ask in what way do these sites particpate with one another in generation of that function. There are two possibilities for the nature of the pathways by which regulatory information is communicated energetically from site to site in a macromolecule:

One possibility is by *indirect pathways*, wherein energetic communication between two functionally important sites is mediated through some other part of the molecule but where the two sites themselves are not directly coupled to one another. Such an effect might involve a simple "triangulation pathway" through a third residue site or could be manifested by a global mechanism wherein overall changes in conformation or solvation are propagated throughout an interface, a domain, or the entire molecule.

† This work was supported by NIH Grants R37-GM24486 and HL-40453 and NSF Grant DMB86-15497.
* To whom correspondence should be addressed.
‡ Present address: Department of Chemistry, University of Wisconsin, Madison, WI 53706.
§ Present address: Dipartmento Scienze e Tecknologie Biomedicke, Ospedale San Raffaele, Milano, Italy.
‖ Present address: Department of Biochemistry and Molecular Biophysics, Washington University School of Medicine, St. Louis, MO 63110.

0006-2960/90/0429-9771$02.50/0

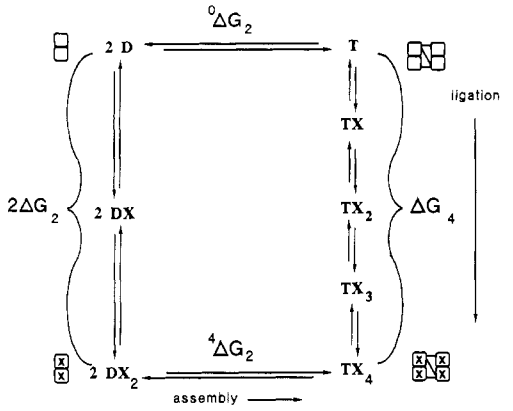

FIGURE 1: Thermodynamic linkage between dimer–tetramer assembly and ligation in human hemoglobin. The left side of the scheme depicts the ligation of $\alpha\beta$ dimers while the right side shows ligation of the tetramers. Since the dimers bind ligands noncooperatively, the difference between the binding free energies of the tetramers versus the dimers is the free energy of cooperativity. By conservation of energy, the free energy of cooperativity is also equal to the difference in dimer to tetramer assembly free energies in the unligated versus the ligated states, i.e., the free energy difference between the top and bottom reactions on the linkage scheme.

The other possibility is by *direct long-range pathways*, wherein two residue sites within the molecule directly communicate energetically in bringing about the functional process. The most extreme form of a direct long-range pathway would be a "chain" of pairwise interactions connecting two sites.

These two classes of communication pathways represent opposite extremes. An allosteric mechanism can in principle consist of any combination of indirect and direct energetic couplings. Experimental determination of the actual combination of communication pathways used by a protein is a step toward understanding how allosteric proteins work.

Human hemoglobin has been studied extensively in this laboratory as a model for understanding mechanisms of energy transduction within macromolecules. The hemoglobin tetramer consists of two identical $\alpha\beta$ dimers. Dissociation of tetramers into $\alpha\beta$ dimers eliminates cooperative ligand binding in hemoglobin, i.e., dimers bind ligands noncooperatively (Mills et al., 1976). Dimer to tetramer association of human hemoglobin can be used as a quantitative tool for studying the free energy of cooperative ligand binding. Figure 1 shows the thermodynamic linkage between ligand binding and subunit assembly in human hemoglobin in simplified form (Ackers & Halvorson, 1974; Mills et al., 1976). By conservation of energy:

$$\Delta G_4 - 2\Delta G_2 = {}^4\Delta G_2 - {}^0\Delta G_2 = \Delta G_c$$

where ΔG_c is the cooperative free energy of ligand binding, i.e., the free energy utilized by the molecule to modify the stepwise binding free energies for the four ligands from their intrinsic values. One approach for addressing the problem of structure–function correlation in the cooperative ligand binding of human hemoglobin is to assess the cooperativity energetics of naturally occurring variants of human hemoglobin and chemically modified human hemoglobins. By assaying the functional effects of numerous specific structural modifications throughout a protein, one obtains information on the structural locations of functional events and the pathways of functional coupling within the molecule. This general strategy has been designated "mapping by structure–function perturbation" (Ackers & Smith, 1985, 1986). This approach has been used to determine that regulation of ligand binding affinity in human hemoglobin is largely due to free energy changes of interactions within the $\alpha^1\beta^2$ interface that are altered upon oxygenation (Pettigrew et al., 1982; Ackers & Smith, 1985, 1986).

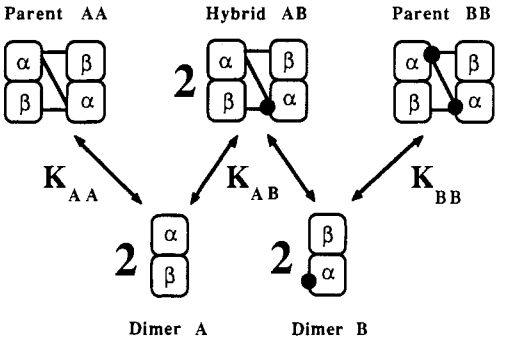

FIGURE 2: A mutant hybrid equilibrium. A mixture of two types of hemoglobin produces an equilibrium consisting of the two "parent" tetramers AA and BB, the hybrid tetramer AB, and the constituent $\alpha\beta$ dimers A and B. The equilibrium is governed by the three constants K_{AA}, K_{AB}, and K_{BB}. A topological convention for depiction of the α and β subunits is also indicated. Tetramer AA in these experiments is the reference tetramer which is either hemoglobin A_0 or S. Here the tetramer BB is an α mutant.

A mutant or chemical variant of human hemoglobin will, because the tetramer consists of two $\alpha\beta$ dimers, have either two altered α residues or two altered β residues. In order to determine how such symmetric perturbations are functionally coupled to one another, we have constructed a series of hybrid hemoglobin tetramers. These hybrids consist of one $\alpha\beta$ dimer from each of two different "parent" molecules. By combining a dimer having no $\alpha^1\beta^2$ interfacial modifications with one that does have such a structural modification, we construct a tetramer containing a single site structural modification within the $\alpha^1\beta^2$ interface. By determining whether or not the singly modified hemoglobin is exactly half as energetically perturbed as the molecule with two symmetric modifications, we are assaying whether the functional effects of modification at the two sites are independent or are energetically coupled.

Such asymmetric hybrid hemoglobins cannot be studied in isolation since their dissociation and reassociation will always lead to establishment of a more complex hybrid equilibrium of the type depicted in Figure 2. We have therefore developed several methods for analysis of such hybrid equilibria (Ackers & Smith, 1986; Smith, 1985; Grasberger et al., in preparation). The most recent and most sensitive of these is quantitative cryogenic isoelectric focusing (QC-IEF).[1]

Electrophoretic and isoelectric focusing studies on hybrid equilibria of the type illustrated in Figure 2 have been carried out by several research groups (Park, 1970, 1973; Bunn & McDonough, 1974; Bunn, 1981; Ip & Asakura, 1984, 1986; Anbari et al., 1985). Accurate quantitation in these systems was difficult, if not impossible, due to the fact that the hybrid system was continuously perturbed away from equilibrium during the separation procedures used. When possible at all, quantitation involved extrapolations to zero separation time (Ip & Asakura, 1984, 1986; Anbari et al., 1985). Perrella and colleagues circumvented this continuous rearrangement by developing new, low-temperature isoelectric focusing and gel electrophoresis technology (Perrella et al., 1978, 1983; Perrella & Rossi-Bernardi, 1981). We have taken advantage of this technology in developing a highly precise and accurate thermodynamic assay, including the relevant theory for resolving the fractional populations of hemoglobins determined by

[1] Abbreviations: QC-IEF, quantitative cryogenic isoelectric focusing. The colloquial abbreviations "deoxy" and "oxy" are used interchangeably with deoxygenated and oxygenated, respectively.

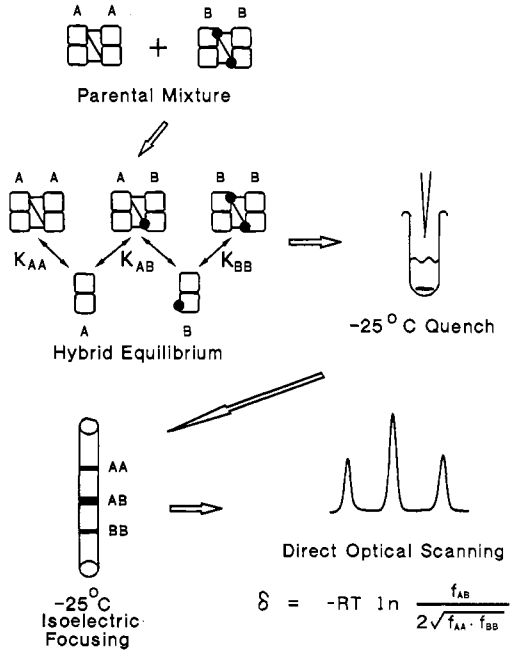

FIGURE 3: Schematic depiction of the steps involved in quantitative cryogenic isoelectric focusing (QC-IEF). See text for details.

QC-IEF in terms of the free energies governing asymmetric hybrid equilibria. Studies of a number of asymmetric mutant hybrid hemoglobins have provided evidence that a combination of indirect and direct long-range pathways of energy transduction operate within the hemoglobin tetramer.

Experimental Procedures

A general schematic representation of the sequence of steps for a quantitative cryogenic isoelectric focusing (QC-IEF) experiment on an asymmetric hybrid hemoglobin system is presented in Figure 3. Individual steps in the procedure are discussed below.

Preparation of Hemoglobins. Hemoglobin A_0 was prepared by the method of Williams and Tsay (1973). The mutant and chemically modified hemoglobins used in this and other site-specific structure modification studies in our laboratory have all been generous gifts donated by numerous benefactors over the past 10 years. Variant hemoglobins were purified via standard ion-exchange chromatography methods for abnormal hemoglobins [cf. Schroeder and Huisman (1980)]. The exact conditions for purification varied depending upon the specific hemoglobin involved. Purified hemoglobins are stored immersed in liquid nitrogen until use. All incubations described herein were carried out in a "standard analytical buffer" consisting of 0.1 M Tris, 0.1 M NaCl, and 1 mM EDTA, pH 7.40 at 21.5 °C. The concentration of Cl^- after adjusting the pH of the buffer is 0.18 M. Hemoglobins used in this study were exchanged into "standard analytical buffer" by using a centrifugal gel permeation technique (Penefsky, 1977).

Incubations. Parental hemoglobins are mixed in the desired proportions at total hemoglobin concentrations between 0.3 and 3.5 mM heme, in a total volume of 20–30 μL, and are incubated for various amounts of time required to reach equilibrium with their hybrid hemoglobins. All incubations are carried out at 21.5 °C in the "standard analytical buffer" described above. Oxy incubations are all performed in microfuge tubes equilibrated in air. Deoxygenated hybrid equilibria must be studied as a function of time to ensure that the system is at equilibrium since the "deviation free energies" determined in this study have no meaning other than at equilibrium. Deoxy incubations are carried out in one or more of the following ways: (1) separate deoxygenation of parent hemoglobins followed by mixing inside a nitrogen-filled glovebag and incubation inside the glovebag; (2) the same as method no. 1 except incubation is carried out in a sealed double vial, i.e., a septum-sealed vial within a crimp-sealed serum vial; (3) the same as no. 2 only in the presence of 0.1% sodium dithionite as an oxygen scavenger; (4) the same as no. 2 only in the presence of 4% "Oxyrase" and 2 mM sodium lactate as an oxygen scavenger; (5) parent hemoglobins are mixed in the oxygenated form, taken inside the glovebag, and deoxygenated by and incubated in the presence of the "Oxyrase" oxygen scavenger system. The "Oxyrase" enzyme system is an oxygen-reducing membrane fraction isolated from *Escherichia coli*. Sodium lactate is used as the hydrogen donor for oxygen reduction. "Oxyrase" is obtained from Oxyrase Inc., Ashland, OH, and is stored frozen until immediately before use. Method no. 5 proves to be the easiest way to perform deoxy incubations and was used for most of the deoxy hybrids described herein. Comparative controls performed with several of the hybrids studied indicate that all five incubation procedures yield equivalent results.

At present the QC-IEF technique is used solely as an equilibrium technique. The thermodynamic validity of the technique in analyzing equilibria of the type shown in Figure 2 does not depend on the kinetics of the approach to equilibrium, so long as the incubation mixture is at equilibrium. The incubation mixture is determined to be at equilibrium when the value of the deviation free energy (δ) plateaus with respect to time [see also LiCata (1990)].

Quenching of Hemoglobins. Hemoglobin incubation samples are quenched into a solution consisting of 50% ethylene glycol and 50% aqueous buffer which has been equilibrated with carbon monoxide at room temperature and is at −26 °C at the time of quenching. The buffer is usually the same "standard analytical buffer" used for incubation of hemoglobins (pH is determined at 21.5 °C).

Quench buffer is placed in a 3.7-mL, 45 mm long screw cap vial, which has a rubber septum in the cap. The vial is submerged approximately 40 mm into a Neslab KT-50 water bath which is regulated at −26 °C. The quench buffer is continuously and rapidly stirred by means of a submersible stir motor. Both oxy- and deoxyhemoglobin hybrid incubations are quenched into the vials by using Hamilton syringes. The ratio of hemoglobin to quench buffer is always 0.1 or smaller.

Preparation of Gels. Polyacrylamide gels for low-temperature isoelectric focusing are prepared essentially as described by Perrella et al. (1981), with some modifications suggested by Dr. M. Samaja (personal communication). The gels are 4.0% polyacrylamide (w/v), 0.16% bis (w/v), 0.154 M ethyl acrylate, 2.47% pH 6–8 ampholytes, 20.6% ethylene glycol, 15.4% methanol, 17.2 mM TEMED, and 0.18% ammonium persulfate (w/v). Acrylamide and bis(acrylamide) are purchased as premade solutions from National Diagnostics. TEMED and ammonium persulfate are electrophoresis grade from Bio-Rad. Ethylene glycol and methanol are "Baker analyzed" grade or better from Baker. Ampholytes are from LKB-Pharmacia (LKB Ampholines). Ethyl acrylate is purum grade from Fluka. The gels are poured in Pyrex glass tubes which are 4 mm o.d., 2.4 mm i.d., and 11.5 cm long. The tubes are treated before use with Silane A174 (Pharmacia-LKB). Gels are poured to a height of 8.4 cm in the tubes. Once poured, gels are stored refrigerated and used within 1 month.

Cryogenic Isoelectric Focusing. Isoelectric focusing of the incubation mixtures is carried out at −25 °C in a plexiglass electrophoresis cell almost identical with that described by

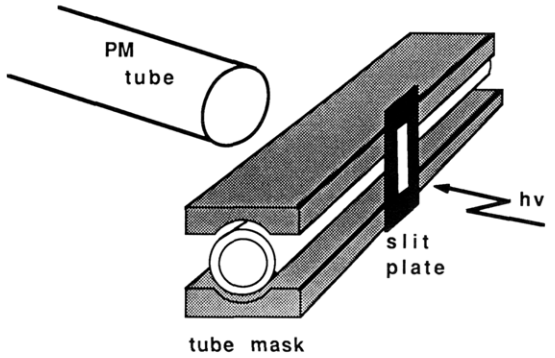

FIGURE 4: Tube holder/mask used for scanning gels. The holder, constructed of a flat black resin, allows reproducibility in positioning of the QC-IEF gel in the Gilford linear transport, helps reduce light scattering and light piping effects, and results in improved precision of scanning.

Perrella et al. (1978, 1981). Plans for building a QC-IEF cell are available from the authors. The cell is kept at −25 °C with the same regulated bath used for the quenching procedure. The cathodic solution (negative electrode) consists of 20% ethylene glycol, 20% methanol, 2% pH 8–9.5 LKB ampholines, and 2% pH 7–9 LKB ampholines. The anodic solution consists of 20% ethylene glycol, 20% methanol, and 0.6% pH 6–8 ampholines. Gels are prerun for 1 h prior to loading samples. Both the prerun and the run itself are performed at 915 V limiting voltage. Amperage per tube generally starts out at 0.2–0.3 mA and decreases within several hours to about $^1/_{10}$ the starting current. Isoelectric focusing is carried out for 20–24 h.

To increase resolution and separation distance between the two parent tetramers and the hybrid tetramer in these IEF gels, we have used hemoglobin S (β6 Glu-Val) as the reference parent tetramer in place of hemoglobin A_0 in these experiments. The amino acid substitution in hemoglobin S occurs at a location on the surface of the molecule and produces a larger p*I* difference between the three tetramers than is the case for the mutants studied when hybridized with A_0. Hemoglobin S and hemoglobin A_0 have identical free energies of cooperativity and rates of dimerization (Pettigrew et al., 1982), so it serves as an excellent surrogate for hemoglobin A_0 in these experiments. Without the increased p*I* difference resultant from using hemoglobin S, most of the hybrid systems studied do not yield three cleanly separated peaks or bands when focused.

Quantitation of Tetramer Populations. After separation is complete, gels are analyzed by direct optical scanning in a Gilford spectrophotometer, equipped with a Gilford linear transport. Scanning is performed at two wavelengths, generally at 420 and 540 nm. Relative tetramer fractions obtained at the two wavelengths are averaged, and any differences contribute to the reported error. The gel is scanned in the tube. A specially constructed holder is used to position the tube properly in the linear transport and to mask the tube to reduce light piping and scattering (see Figure 4). Plans for building such a holder are available from the authors. Absorbance readings are collected directly onto an HP150 computer via an HP digital multimeter which is connected to the voltage output of the spectrophotometer. Calculation of the fractional areas of each of the three peaks is performed via trapezoidal integration of the collected data. In order to handle cases where absorbance values do not return completely to base line between peaks, definition of peaks is carried out via both valley to valley and by dropline techniques (see Figure 5). Any differences resulting from defining the peaks in these two ways are reflected in the standard deviation (σ) of the determined free energies of deviation from additivity (δ). Any minor peaks that appear in the scans (corresponding to possible impurities in the hemoglobins or Met formation during long incubations) are included in the total integrated area and again are reflected in the reported error for any hybrid.

The techniques for data collection and integration described above are those presently in use in this laboratory. We have, however, with equal success, utilized less streamlined techniques. Manual integration by polar planimetry of scans collected on a Varian chart recorder, collection of scans on an analog integrating chart recorder, and collection and electronic integration on an LKB Model 2220 recording integrator all provide equally acceptable quantitation of the values of f_{AA}, f_{AB}, and f_{BB} in a cryogenic isoelectric focusing experiment.

THEORY

In this section we present theoretical relationships for determination and analysis of the free energies of the hemoglobin mutant hybrid systems we are studying. Section I illustrates the connection between experimental results and the free energies governing the hybrid equilibrium. Section II discusses the results of simulations aimed at determining the energetic range of applicability of the equations presented in Section I. Section III presents a theoretical framework for interpretation of the obtained hybrid system free energies. These approaches are generally applicable for structure–function perturbation studies in any polymerizing system where hybrid or mixed-subunit noncovalent macromolecular assemblies can be formed.

(*I*) *Analysis of Hybrid Equilibria.* When analyzing the energetics of formation of asymmetric hybrid hemoglobins, one must study the hybrid hemoglobin in complex equilibria of the type shown in Figure 2.

Disproportionation reactions prevent isolation of the hybrid species AB. One can relate the concentrations of each of the five molecular species present at equilibrium to the three constants governing the equilibrium via the simultaneous equations:

$$C_A = 2[A] + 4K_{AA}[A]^2 + 2K_{AB}[A][B] \quad (1)$$

$$C_B = 2[B] + 4K_{BB}[B]^2 + 2K_{AB}[A][B] \quad (2)$$

where

$$[AA] = K_{AA}[A]^2$$

$$[BB] = K_{BB}[B]^2$$

$$[AB] = K_{AB}[A][B]$$

Here, and in all of the equations presented herein, "A" and "B" represent two different types of $\alpha\beta$ hemoglobin dimers while "AA", "AB", and "BB" represent the three tetramers formed by assembly of A and B type dimers. Each of the three tetramers AA, AB, and BB has its own characteristic dimer to tetramer assembly constant K_{AA}, K_{AB}, and K_{BB}, respectively. C_A and C_B represent the total concentrations of A and B type dimers in the hybrid equilibrium, whether present as free dimers or as part of a tetramer, expressed in molar heme (which accounts for the factors of 2 and 4 in eqs 1 and 2). Numerical solution of these equations allows prediction of the concentrations of all three tetramers and both dimers at equilibrium from a knowledge of the three equilibrium constants plus the concentrations of each of the parent hemoglobins added to form the hybrid equilibrium (C_A and C_B).

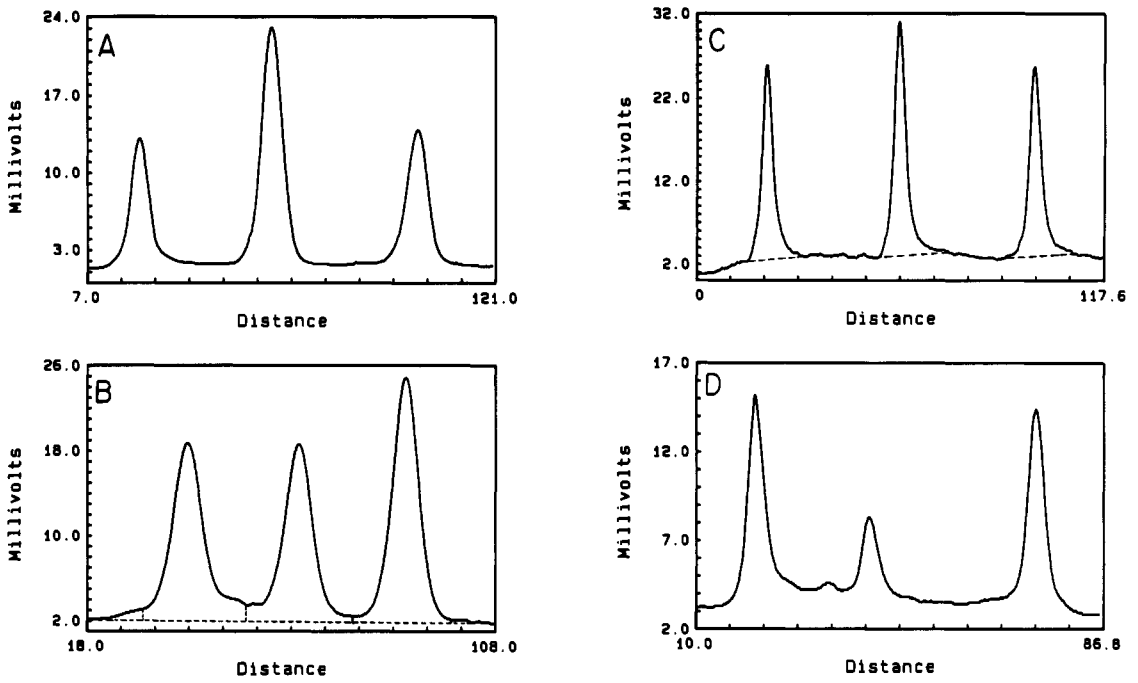

FIGURE 5: Representative scans of several QC-IEF gels. (A) Deoxygenated A/S scanned at 540 nm, δ = 0.14 kcal/mol; (B) deoxygenated S/Kempsey scanned at 420 nm, δ = 0.52 kcal/mol; (C) oxygenated S/desArg scanned at 420 nm, δ = 0.25 kcal/mol; (D) oxygenated S/St. Calude scanned at 540 nm, δ = 0.91 kcal/mol. All scans are oriented anodic to cathodic so that in each tube the mutant parent is the leftmost peak (lowest X-axis position number), the hybrid is in the middle, and hemoglobin S is the rightmost peak. In scan A, hemoglobin A_0 is the leftmost peak. The scans are all on different scales. Since one is quantitating the relative fractional areas, the absolute scales are unimportant. Critical requirements are as follows: (1) the rate at which the gel is passed through the light beam is constant, and (2) the scans are performed within an optical density range of sufficient linearity. Points along the x axis are collected in discrete time intervals as the gel is passed through the light beam of the spectrophotometer. Between 800 and 1600 data points are collected depending on the distance of separation between the hemoglobins on the gel and the rate at which the gel is scanned. In these figures the x axis is labeled with position numbers that are proportional to different distances along the gel depending on the rate at which a gel is scanned. Optical density is recorded in millivolts and integration is performed without conversion. The voltage output of the Gilford spectrophotometer is proportional to absorbance. Most scans are performed on a scale where 10 mV = 0.44 OD. Since it is sometimes difficult to decide where a particular peak begins or ends, because of trailing effects, etc., peaks are sometimes cut in several different places and reintegrated. The two techniques used for peak definition for integration of scans of cryo-IEF gels are also shown in this figure. In scan B the dropline technique is shown, while scan C shows the trough-to-trough technique. All scans are integrated by using both techniques.

One can also write the relationship between the tetramer concentrations and the three equilibrium constants as

$$\frac{2K_{AB}}{\sqrt{K_{AA}K_{BB}}} = \frac{[AB]}{\sqrt{[AA][BB]}} \quad (3)$$

Note that a statistical factor of 2 is required to balance the equation properly. Then, since [AA] + [AB] + [BB] = the total concentration of tetramer at equilibrium, by substitution one obtains

$$\frac{2K_{AB}}{\sqrt{K_{AA}K_{BB}}} = \frac{f_{AB}}{\sqrt{f_{AA}f_{BB}}} \quad (4)$$

This equation rigorously relates the relative fractions of each of the three tetramers at equilibrium to the three equilibrium constants for the hybrid equilibrium. Using eq 4, one can determine any one of the three equilibrium constants given the other two plus the relative fractions of the three tetramers. Since the parent tetramers AA and BB can be studied in isolation by other techniques (Ip et al., 1976; Turner et al., 1981), one uses eq 4 to determine the free energy of formation for the hybrid hemoglobin AB.

When using eq 4 as described above, one introduces experimental error from the determination of the tetramer fractions f_{AA}, f_{AB}, and f_{BB}, as well as propagating the error in the independent determinations of K_{AA} and K_{BB}. The QC-IEF technique, however, directly yields a thermodynamic quantity we call the "deviation free energy", which is independent of the values of K_{AA} and K_{BB}.

If the free energy of assembly of tetramer AB from dimers is equal to the mean of the assembly free energies of its parent molecules AA and BB, we say the hybrid molecule is energetically *additive*:[2]

$$\Delta G^{AB}_{add} = \tfrac{1}{2}(\Delta G^{AA}_{expt} + \Delta G^{BB}_{expt}) \quad (5)$$

The free energies, again, correspond to the reactions depicted in Figure 2. Such an additive molecule would result in a binomial distribution of f_{AA}:f_{AB}:f_{BB} = 1:2:1 at equilibrium, according to eq 4, when the parents are mixed in equal initial proportions. If the assembly free energy of hybrid AB is not the mean of its parents, then we say the hybrid is *nonadditive* and define the deviation free energy δ as the difference between the actual hybrid assembly energy and the additive hybrid assembly energy:

$$\delta = \Delta G^{AB}_{expt} - \Delta G^{AB}_{add} \quad (6)$$

By substitution of eqs 4 and 5 into eq 6, we get

$$\delta = -RT \ln \frac{f_{AB}}{2\sqrt{f_{AA}f_{BB}}} \quad (7)$$

[2] Abbreviations used as superscripts and subscripts in equations in this section include the following: add = additive, expt = experimental, mut = mutant, ref = reference, hyb = hybrid, eq = at equilibrium, init = initial, AA = parent tetramer AA, AB = the hybrid tetramer, BB = parent tetramer BB, t = tetramer, d = dimer, and i = ligation state index. These conventions have the same meaning whether they appear as subscripts or as superscripts.

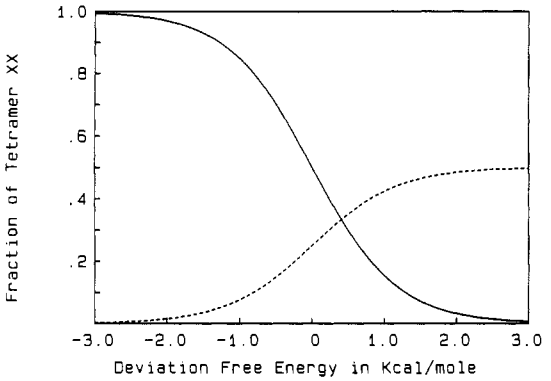

FIGURE 6: Relationship between the equilibrium fractions of the three tetramers AA, BB, and AB and the deviation free energy, δ, for a 1:1 initial mixture of AA and BB. The solid line denotes the fraction of hybrid (f_{AB}) while the dashed line shows the parent tetramer fractions f_{AA} and f_{BB}, which are identical in a 1:1 initial proportion experiment. A deviation free energy of zero corresponds to an additive hybrid system and a binomial distribution of tetramers AA, AB, and BB (1:2:1). A positive δ indicates that the hybrid is destabilized relative to the mean of its parents' free energies of assembly.

The deviation free energy, δ, is measured directly by the QC-IEF method and is completely independent of the absolute values of the three equilibrium constants K_{AA}, K_{AB}, and K_{BB}. Figure 6 shows the relationship between the equilibrium tetramer fractions and the deviation free energy of the hybrid for a 1:1 initial mixture of parents AA and BB at 21.5 °C. Numerical solution of the simultaneous eqs 1 and 2 will yield functions analogous to Figure 6 for any values of the equilibrium constants. Figure 6 and eq 7 represent the most general form of this relationship and hold for any combination of K_{AA}, K_{AB}, and K_{BB}.

Figure 6 shows simulated results for hybrid systems in which the parent tetramers AA and BB are mixed in equal proportions. Equations 1–7 above hold, however, for any initial proportions of AA and BB. Additionally, one can analytically relate the equilibrium fractions of hemoglobin tetramers AA, AB, and BB to their initial fractions AA^{init} and BB^{init} for any ratio AA^{init}:BB^{init} if one knows the deviation free energy of the hybrid:

for $\delta = 0$

$$f_{AB}^{eq} = 2(f_{AA}^{init} f_{BB}^{init}) \tag{8}$$

for $\delta \neq 0$

$$f_{AB}^{eq} = \frac{N - \sqrt{N^2 - 4N^2(f_{AA}^{init} f_{BB}^{init}) + 4N(f_{AA}^{init} f_{BB}^{init})}}{N - 1} \tag{9}$$

$$N = \frac{K_{AB}^{\ 2}}{K_{AA}K_{BB}} = e^{(-2\delta/RT)}$$

for both $\delta = 0$ and $\delta \neq 0$

$$f_{AA}^{eq} = f_{AA}^{init} - \tfrac{1}{2}f_{AB}^{eq} \qquad f_{BB}^{eq} = f_{BB}^{init} - \tfrac{1}{2}f_{AB}^{eq}$$

These equations are illustrated graphically in Figure 7 and are discussed further in section II below. Any hybrid system of the type illustrated in Figure 2 at equilibrium must follow the relationships illustrated by Figure 7 and eqs 1, 2, 8, and 9. Mixing parent hemoglobins in different proportions is therefore a powerful control for thermodyanmic validity of the quantitative cryogenic isoelectric focusing technique.

A special property of δ lies in its dependence on properties of the tetrameric molecules alone; i.e., if ΔG^{AB} denotes the free energy of assembly of tetramer AB, then

$$\Delta G^{AB} = G_{tet}^{AB} - G_{dimer}^{A} - G_{dimer}^{B} \tag{10}$$

where the terms on the right denote free energies of the respective species that participate in the reaction. Substituting these terms (and the corresponding ones for ΔG^{AA} and ΔG^{BB}) into eqs 5 and 6, we see immediately that

$$\delta = G_{tet}^{AB} - \tfrac{1}{2}(G_{tet}^{AA} + G_{tet}^{BB}) \tag{11}$$

These are the chemical potentials of the tetramers alone, relative to any chosen reference state.

(II) Simulation Studies. Equations 3–9 rigorously relate the fractional populations of tetrameric hemoglobins to the relative dimer to tetramer association free energies of all the species in an asymmetric hybrid equilibrium. In QC-IEF experiments preformed on asymmetric hybrid hemoglobins one obtains three focused bands, or peaks, at equilibrium (see Figure 5). Simulation studies show that in general one may directly use the fractional masses as determined by absorbance scans of the three experimentally obtained hemoglobin peaks as the f_{AA}, f_{AB}, and f_{BB} values used to calculate the deviation free energy of the hybrid system. This approach essentially assumes that $\alpha\beta$ dimers do not interfere with the quantitation of the three tetramer fractions. Simulations show this assumption to be valid at the concentrations of hemoglobin used in these experiments to within ±0.1 kcal/mol or better for the calculated deviation free energy δ when all three tetramers have dimer to tetramer association free energies on the order of −6.5 kcal/mol or tighter. This is because the total concentration of hemoglobin in a cryogenic isoelectric focusing experiment is such that the concentrations of the two dimers A and B are on average several orders of magnitude lower than the concentration of tetramers. Performing experiments at higher concentrations of hemoglobin increases the range of validity. All but two of the hybrid systems examined in this study (oxygenated S/Austin and oxygenated S/Athens GA) meet the criteria for direct application of eqs 3–9 to the three peaks determined by experiment.

Simulations are performed by comparing predicted experimental results generated by using eqs 1 and 2 with predicted experimental results generated by using eqs 8 and 9 for any particular set of equilibrium constants K_{AA}, K_{AB}, and K_{BB}. For simulations with eqs 1 and 2 total heme concentrations near or matching actual experimental concentrations are used (between 0.3 and 3 mM heme for all hybrid systems studied). Equations 8 and 9 are independent of hemoglobin concentration. Previous studies on asymmetric hybrid systems at temperatures which do not effectively "trap" the system provide evidence that the $\alpha\beta$ dimers probably focus with their like parents (Park, 1973; Bunn & McDonough, 1974; Bunn, 1981). For simulations with eqs 1 and 2 we assume all dimers focus with their parent tetramers, such that the three peaks resolved by isoelectric focusing would correspond to ([AA] + [A]), [AB], and ([BB] + [B]).

Figure 7 shows two examples of the results of these simulations. Figure 7A shows simulated and actual results for the oxygenated A/S hybrid system. In this case the results are effectively the same regardless of where dimers focus (the difference in δ using the two methods is 0.020 kcal/mol). The dimers are present in concentrations too low to significantly alter the calculated δ. This situation holds at the concentrations of these experiments for all hybrid systems where all three tetramers have association free energies tighter than −6.5 kcal/mol regardless of the magnitude of δ. Figure 7B shows simulated and actual results for the oxygenated S/Austin system where, since the association free energy of oxygenated hemoglobin Austin is −4.5 kcal/mol, a relatively large number of dimers will be present to "interfere" with accurate determination of the relative tetrameric fractions. The simulated

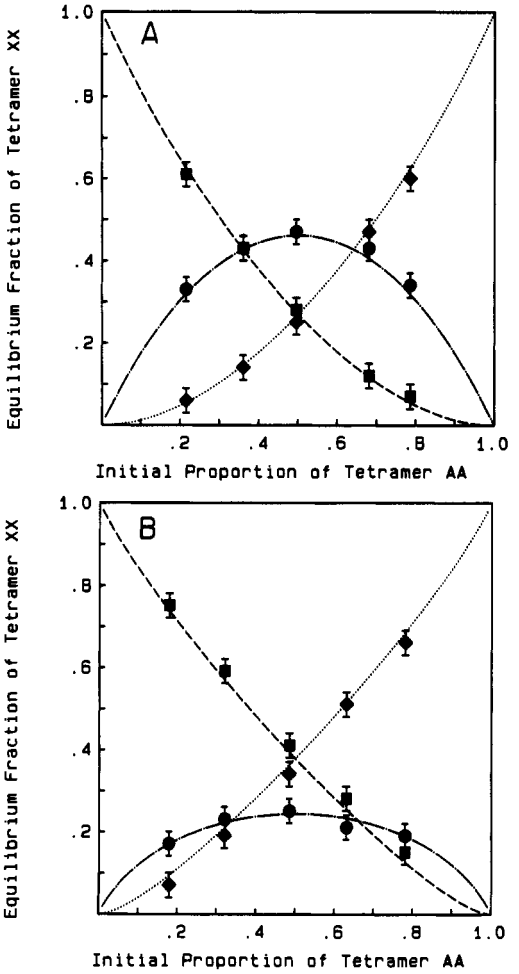

FIGURE 7: Relationship between initial fractions of parent hemoglobins and the equilibrium fractions of AA, BB, and AB. The x axis shows the initial relative fractions of parents expressed as the fraction of tetramer AA added, while the y axis shows the equilibrium fractions for the resulting three tetramers in the hybrid equilibrium. The lines are simulated data for particular values of δ generated by using eqs 1 and 2, and eqs 8 and 9, as described in the text. The symbols show the experimental results for mixing different initial proportions of parent hemoglobins. In both graphs, the lines are simulated data and the symbols are actual data. In both graphs, the dashed line and the squares (■) denote the fraction of the mutant tetramer f_{BB}; the dashed-dotted line and the circles (●) denote the fraction of hybrid f_{AB}; and the dotted line and the diamonds (♦) denote the fraction of the reference parent f_{AA}. (A) Shown here is the oxygenated A/S hybrid system. For any hybrid system where all three tetramer association free energies are tighter than −6.5 kcal/mol, the presence or absence of dimers is negligible in the millimolar concentration ranges in which the experiments are performed. The simulated lines represent a δ of 0.0920 kcal/mol with (using eqs 1 and 2) or 0.090 kcal/mol without (using eqs 8 and 9) "interfering" dimers. (B) For cases where one or more of the tetramers in the hybrid equilibrium is highly dissociated one finds dimers interfere with accurate quantitation of the tetrameric fractions. Shown is the case for oxygenated S/Austin where the simulated lines represent a δ of 0.2 kcal/mol when dimers are assumed to focus with their like parents, and a δ of 0.66 kcal/mol if the three peaks are considered to represent only the tetrameric fractional populations. Without knowing exactly where dimers focus on the QC-IEF gels, one cannot distinguish which of these two possibilities correctly describes the energetics of the system. In the two cases where interfering dimers create such an imprecision we report the error on δ as covering the entire range of this uncertainty.

lines show the fit to the data using eqs 1 and 2 ($\delta = 0.20 \pm 0.23$ kcal/mol) and using eqs 8 and 9 ($\delta = 0.66 \pm 0.23$ kcal/mol). Similar simulations for the S/Athens GA oxygenated hybrid system were performed to determine the error on the δoxy in Table I. Simulations for the oxygenated S/St. Mande hybrid system ($^4\Delta G_2$ for St. Mande = −6.4 kcal/mol)

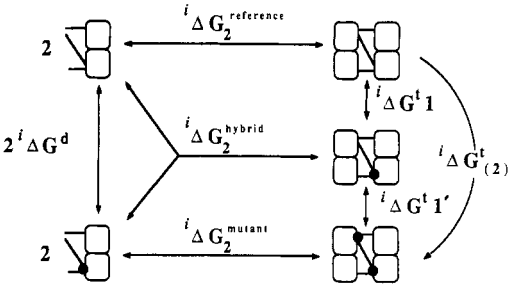

FIGURE 8: Thermodynamic linkage between structural modification of hemoglobin and dimer–tetramer assembly energetics. Relationships illustrated in this linkage diagram are used in the text to examine the differential energetic effects of two structural modifications, and to show that the perturbation free energies and deviation free energies are properties of the tetrameric species.

show that at the concentration of the experiment the calculated δ does not change by more than 0.1 kcal/mol whether the $\alpha\beta$ dimers interfere or not.

(III) Interpretation of δ Values. The general rationale for detecting direct long-range coupling using the strategy of mapping by structure–function perturbation is as follows: Consider a protein P which undergoes a function characterized by a free energy F. For single site variants of P, P_1 and P_2, the corresponding *functional perturbations*, will be δF_1 and δF_2. For the molecular species P_{12} (containing both structural modifications), one can assay the independence of the perturbations caused by the modifications at sites 1 and 2 via the relationship: $\delta F_{12} = \delta F_1 + \delta F_2$. If this equality does not hold, this provides evidence that the two sites are directly coupled in generating the functional response F. If this equality holds, then, except for coincidences, the two sites are independent of each other in generating the function F. The two sites may still be on the functional pathway which manifests F, however. If the functional perturbation energies δF_1 and δF_2 are nonzero and the equality holds, then the two sites are on the functional pathway for F, yet are independent of each other, and are therefore coupled indirectly in a "triangular" or global manner. These general relationships are discussed at length in Ackers and Smith (1985, 1986). Application of these general strategies to the study of energetic coupling during cooperative ligation using asymmetric mutant hybrid hemoglobins where only one of the parent molecules is functionally perturbed is relatively straightforward. We develop this application in detail for the remainder of this section. It should be noted that the structural modifications we are dealing with are sufficiently small that the overall structure of the tetrameric molecules are similar, yet the magnitudes of functional perturbations are in the same range as in oxygen binding to the normal molecule.

Note also that in the hybrid systems of the type examined in this paper the two structural modifications are "identical". Hence we denote the individual site functional perturbation free energies as δF_1 and $\delta F_1'$. The thermodyanmic linkage depicted in Figure 8 shows the relationship between the dimer to tetramer assembly free energies for the three tetramers involved in a mutant hybrid equilibrium and the free energies of introducing the structural modifications into the dimer (ΔG^d) and into the tetramer ($\Delta G^t_{(2)}$, where $\Delta G^t_{(2)} = \Delta G^t1 + \Delta G^t1'$). We can use the linkage of Figure 8 to determine the energetic perturbation to the *function* of dimer–tetramer assembly resulting from the structural modifications. We define $\delta F_{(2)}$ as the functional perturbation caused by a pair of symmetric structural modifications:

$$^i\delta F_{(2)} = {}^i\Delta G^t_{(2)} - 2\,{}^i\Delta G^d = {}^i\Delta G_2^{mut} - {}^i\Delta G_2^{ref} \quad (12)$$

Here i is an index for the ligation state of the molecule: i = 0 for deoxyhemoglobin and i = 4 for oxygenated hemoglobin. The reference free energy is always that of hemoglobin A_0 (or hemoglobin S which has values of ${}^0\Delta G_2$ and ${}^4\Delta G_2$ identical with those of hemoglobin A_0). Note that the superscripts ref(erence), mut(ant), and hyb(rid) replace AA, BB, and AB here and throughout much of this section. AA, BB, and AB are used to denote any two parent tetramers and the hybrid between them, while ref, mut, and hyb refer specifically to a functionally unperturbed parent, a functionally perturbed parent, and the hybrid between them, respectively.

By analogy we can define the functional perturbations resulting from each of the two "identical" single site modifications:

$$ {}^i\delta F_1 = {}^i\Delta G^t1 - {}^i\Delta G^d = {}^i\Delta G_2^{hyb} - {}^i\Delta G_2^{ref} \quad (13) $$

$$ {}^i\delta F_1' = {}^i\Delta G^t1' - {}^i\Delta G^d = {}^i\Delta G_2^{mut} - {}^i\Delta G_2^{hyb} \quad (14) $$

In analyzing a hybrid equilibrium, one determines two of the three quantities: ${}^i\delta F_{(2)}$ and ${}^i\delta F_1$, (${}^i\delta F_1'$ is then derived from these two values). Therefore, in order to test for direct long-range coupling in this system, we set ${}^i\delta F_1 + {}^i\delta F_1' = {}^i\delta F_{(2)}$ and assay for independence of sites via the relationship ${}^i\delta F_1 = {}^i\delta F_1'$ (which is equivalent to the relationship ${}^i\delta F_{(2)} = 2{}^i\delta F_1$). If this equality does not hold, it provides evidence that the two residues are energetically coupled to one another in generating the functional response; they "detect one another's presence"; their effects are cooperative. If ${}^i\delta F_1 = {}^i\delta F_1'$ and the two quantities are nonzero, then the two sites are indirectly coupled in generating the function.

Equations 13 and 14 can be combined to yield the important relationship:

$$ {}^i\delta F_1 - {}^i\delta F_1' = {}^i\Delta G^t1 - {}^i\Delta G^t1' = 2{}^i\Delta G_2^{hyb} - {}^i\Delta G_2^{ref} - {}^i\Delta G_2^{mut} = 2\delta^i \quad (15) $$

This equation relates δ to the functional perturbation energies associated with the two site-specific structural modifications involved in the hybrid equilibrium. The quantity δ obtained by QC-IEF is a direct measure of whether ${}^i\delta F_1 = {}^i\delta F_1'$ and hence of the direct coupling of the two symmetric sites. This equation like eq 11 also demonstrates that the deviation free energies we observe for the mutant hybrid hemoglobins studied are solely a property of the tetrameric molecule.

The individual site functional perturbation free energies ${}^i\delta F_1$ and ${}^i\delta F_1'$ are calculated by using the values of δ determined by QC-IEF and the values of ${}^0\Delta G_2$ and ${}^4\Delta G_2$ for each of the mutant hemoglobins studied via eq 12 and the equations:

$$ {}^i\delta F_1 = \frac{{}^i\delta F_{(2)}}{2} + \delta^i \quad (16) $$

$$ {}^i\delta F_1' = \frac{{}^i\delta F_{(2)}}{2} - \delta^i \quad (17) $$

Table II shows the differential functional perturbation free energies ${}^i\delta F_1$ and ${}^i\delta F_1'$ for both the deoxy (i = 0) and oxy (i = 4) ligation states of the the mutant hybrid systems studied by QC-IEF. The propagated errors on the values of ${}^i\delta F_1$ and ${}^i\delta F_1'$ can be very large since they include the errors on ${}^i\Delta G_2$ for both the mutant and the reference hemoglobins and the error on δ. However, these transformations of δ are used here as an interpretative framework based on the statistically significant differences in the δ values.

The thermodynamic linkage shown in Figure 8 is for a single ligation state, either oxygenated or unligated. The cooperative free energy of ligand binding of any hemoglobin is equal to the difference in its dimer to tetramer assembly free energies in the unligated and ligated states:

$$ \Delta G_c = {}^4\Delta G_2 - {}^0\Delta G_2 \quad (18) $$

Then, to calculate the differential effect of the two perturbations on the cooperative free energy:

$$ \delta^{coop} = \delta oxy - \delta deoxy \quad (19) $$

Additionally, it can be seen from eqs 11 and 19 that

$$ \delta^{coop} = \Delta G_4^{AB} - \tfrac{1}{2}(\Delta G_4^{AA} + \Delta G_4^{BB}) \quad (20) $$

where each ΔG_4 term represents the free energy of oxygenation for the respective tetrameric species. We thus see that δ^{coop} describes the nonadditivity of oxygenation free energies among the tetramers alone, exclusive of all dimeric properties.

By analogy to eqs 16 and 17, we can define cooperativity-linked functional perturbation energies:

$$ \delta\Delta G_c1 = \tfrac{1}{2}(\Delta G_c^{ref} - \Delta G_c^{mut}) - \delta^{coop} \quad (21) $$

$$ \delta\Delta G_c1' = \tfrac{1}{2}(\Delta G_c^{ref} - \Delta G_c^{mut}) + \delta^{coop} \quad (22) $$

As was the case with ${}^i\delta F_1$ and ${}^i\delta F_1'$, the propagated errors on the values of $\delta\Delta G_c1$ and $\delta\Delta G_c1'$ in Table III will be rather large. Again, however, these transformations are included here to assist in interpreting the meaning of δ^{coop}. The propagated error on δ^{coop} in Table III is calculated by using the standard formula: $\sigma^{coop} = [(\sigma^{oxy})^2 + (\sigma^{deoxy})^2]^{1/2}$ (Bevington, 1969).

The key interpretive results of these specific relationships for hybrids of the type examined in this paper are, however, as follows: (1) if the QC-IEF measured value of δ (oxygenated or deoxygenated) is nonzero, then the two symmetric perturbed sites in the hybrid system are directly coupled relative to dimer–tetramer assembly; (2) if δ^{coop} is nonzero, then the two sites are directly coupled in the generation of cooperativity; and (3) if the two sites are independent of each other (δ's are zero), yet they still perturb the function assayed (dimer–tetramer assembly and/or cooperativity), then the two sites are coupled along an indirect pathway in generation of that function.

Results

Quantitative Cryogenic Isoelectric Focusing. The distance between any two hemoglobins on these gels, once they are fully focused, depends, of course, on their relative pI's. Figure 9 shows photographs of several typical gels. The separation between parent hemoglobins on these gels ranges from about 0.8 cm (e.g., S/Radcliffe, S/Kempsey) to just over 3 cm (e.g., S/Chesapeake, S/desArg). Separation distances vary somewhat from run to run depending mostly on the age of the electrode solutions, but the relative positions of course do not change. Since this separation technique is nondenaturing, the relative separation between any two hemoglobins is not always predictable from the known amino acid changes involved.

When hemoglobin S is used as a surrogate for hemoglobin A_0, the separation distances among the three bands on the gel allow for relatively straightforward scanning and quantitation. As can be seen in Figure 5, the species profiles from scans of these IEF gels are typically well resolved. The minimum separation distance between two parent hemoglobins which will allow accurate direct quantitation of the parent peak areas as well as the area of the hybrid between them is about 0.8 cm. There simply is not room for a cleanly separated hybrid peak between the two parent peaks if the separation distance is smaller than this.

Figure 6 shows the change in deviation free energy δ relative to the change in the fractions of the three tetramers at equilibrium for a 1:1 initial mixture of any two hemoglobins. The most sensitive response of the system occurs in the region near "additivity". Here a deviation free energy δ of 0.1

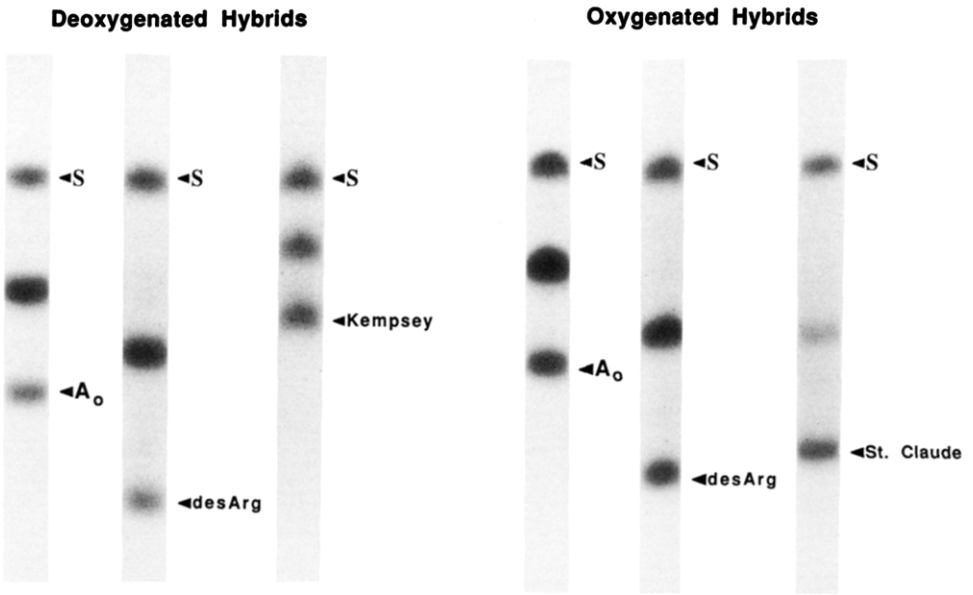

FIGURE 9: Photographs of cryo-IEF separations of hybrid equilibria. On the left are three deoxygenated hybrid equilibria after focusing: A/S, S/desArg, and S/Kempsey. On the right are three oxygenated hybrid systems: A/S, S/desArg, and S/St. Claude. Hemoglobin S is always the uppermost of the three bands (most cathodic), and the hybrid is always the centermost band.

Table I: Deviation Free Energies for Asymmetric Mutant Hybrid Hemoglobins As Determined by Quantitative Cryogenic Isoelectric Focusing[a]

mutant hybrid	position	location	δdeoxy	δoxy
A/S (reference)	β6 Glu-Val	external	0.14 ± 0.11	0.09 ± 0.10
S/Kariya	α40 Lys-Glu	$\alpha^1\beta^2$ interface	0.17 ± 0.12	0.08 ± 0.10
S/Chesapeake	α92 Arg-Leu	$\alpha^1\beta^2$ interface	0.06 ± 0.35	0.12 ● 0.10
S/Dallas	α97 Asn-Lys	$\alpha^1\beta^2$ interface	0.08 ± 0.10	0.06 ± 0.10
S/Tarrant	α126 Asp-Asn	$\alpha^1\beta^1$ and $\alpha^1\alpha^2$	0.12 ± 0.10	−0.08 ± 0.10
S/St. Claude	α127 Lys-Thr	$\alpha^1\alpha^2$ contact	1.35 ± 0.55	0.91 ± 0.43
S/desArg	α141 deleted	$\alpha^1\beta^2$ interface	0.30 ± 0.16	0.25 ± 0.12
S/Austin	β40 Arg-Ser	$\alpha^1\beta^2$ interface	0.43 ± 0.45	0.43 ± 0.46[b]
S/Athens GA	β40 Arg-Lys	$\alpha^1\beta^2$ interface	0.18 ± 0.10	0.09 ± 0.21[b]
A/Zurich	β63 His-Arg	distal histidine	0.22 ± 0.12	0.13 ± 0.18
S/thio-CH_3	β93 Cys	$\alpha^1\beta^2$ interface	0.17 ± 0.11	0.00 ± 0.19
S/NES	β93 Cys	$\alpha^1\beta^2$ interface	0.20 ± 0.17	0.19 ± 0.10
S/Hotel Dieu	β99 Asp-Gly	$\alpha^1\beta^2$ interface	0.26 ± 0.10	0.01 ± 0.10
S/Radcliffe	β99 Asp-Ala	$\alpha^1\beta^2$ interface	0.21 ± 0.10	0.00 ± 0.10
S/Kempsey	β99 Asp-Asn	$\alpha^1\beta^2$ interface	0.52 ± 0.10	−0.01 ± 0.10
S/Yakima	β99 Asp-His	$\alpha^1\beta^2$ interface	0.31 ± 0.10	−0.01 ± 0.10
S/Ypsilanti	β99 Asp-Tyr	$\alpha^1\beta^2$ interface	0.69 ± 0.11	0.06 ● 0.12
S/St. Mande	β102 Asn-Tyr	$\alpha^1\beta^2$ interface	0.39 ± 0.19	0.90 ● 0.23
S/TyGard	β124 Pro-Gln	$\alpha^1\beta^1$ contact	0.09 ± 0.20	0.05 ± 0.11
S/Abruzzo	β143 His-Arg	external	0.21 ± 0.10	0.20 ± 0.10

[a] All values are reported in kcal/mol. All location classifications are according to Sack et al. (1978). All errors are standard deviations except where indicated. [b] The two oxygenated hybrids, for which the error includes the presence of interfering dimers (see Theory, section II).

kcal/mol is reflected in about a 4% change in the population fraction of hybrid tetramer. The result of this fact is that even a small deviation from addivity, say, on the order of 0.25 kcal/mol, is often obvious even by eye with this technique (see Figures 5 and 9).

The deviation free energies δ for several hybrid hemoglobins are given in Table I. The relative precision on the determination of δ varies somewhat among hybrids and is most directly correlated with the purity of the hemoglobin sample. The "cleanest" hemoglobins produce hybrid and parent peak patterns by QC-IEF that have standard deviations (σ) on the calculated value of δ which are significantly below ±0.10 kcal/mol. In Table I all such small σ's have been "rounded up" to ±0.10 kcal/mol.

A large number of controls have been performed to establish thermodynamic validity of the results for the deviation free energies reported in Table I (LiCata, 1990). Separate simultaneous quenching of the two parent tetramers, without mixing them first, yields two instead of three peaks by QC-IEF [data not shown; see also Perrella et al. (1978, 1981, 1983) and Perrella and Rossi-Bernardi (1981)]. Changing the pH or the ionic strength of the quench buffer does not appreciably change the coupling free energy calculated for a hybrid (data not shown). Changing the gas with which one saturates the quench buffer does not appreciably change the δ (data not shown). The method of transfer from the quench buffer to the gels, the time of isoelectric focusing, the wavelength at which one scans the gels: all of these, as well as other possible sources of systematic error, have been explored (LiCata, 1990). Mixing the hemoglobins in different initial proportions serves as an excellent control for systematic perturbation of a hybrid system from equilibrium. Figure 7 shows data for two hybrid systems at different initial proportions as well as the predicted behavior of the hybrid equilibria in the absence of any systematic error. The agreement between predicted and observed behavior for a hybrid system of known δ is evidence that the hybrid equilibrium is not being perturbed by the QC-IEF technique.

Asymmetric Mutant Hybrids. Table I shows the results of studies on 40 hybrid hemoglobins: 20 different hemoglobin

Table II: Functional Perturbation Energies for Asymmetric Mutant Hybrids[a]

mutant hybrid	deoxygenated hybrids			oxygenated hybrids		
	$^0\Delta G_2$[b]	$^0\delta F_1$[c]	$^0\delta F_1'$[c]	$^4\Delta G_2$[b]	$^4\delta F_1$[c]	$^4\delta F_1'$[c]
A/S (reference)	−14.3 ± 0.2	0.1	−0.1	−8.0 ± 0.1	0.1	−0.1
S/Kariya	−9.7 ± 0.1	2.5	2.1	−8.0 ± 0.1	0.1	−0.1
S/Chesapeake	−11.7 ± 0.2	1.4	1.2	−9.6 ± 0.1	−0.7	−0.9
S/Dallas	−11.4 ± 0.2	1.5	1.4	−9.5 ± 0.1	−0.7	−0.8
S/Tarrant	−10.0 ± 0.2	2.3	2.0	−8.2 ± 0.1	−0.2	0.0
S/St. Claude	−11.1 ± 0.1	3.0	0.3	−8.0 ± 0.1	0.9	−0.9
S/desArg	−10.1 ± 0.2	2.4	1.8	−9.0 ± 0.1	−0.3	−0.8
S/Austin	−12.0 ± 0.1	1.6	0.7	−4.5 ± 0.2	2.2	1.3
S/Athens GA	−13.5 ± 0.1	0.6	0.2	−5.4 ± 0.5	1.4	1.2
A/Zurich	−12.9 ± 0.1	0.9	0.5	−6.9 ± 0.2	0.7	0.4
S/thiomethylated	−13.0 ± 0.1	0.8	0.5	−7.2 ± 0.1	0.4	0.4
S/NES	−11.5 ± 0.1	1.6	1.2	−8.5 ± 0.2	−0.1	−0.4
S/Hotel Dieu	−8.2 ± 0.1	3.3	2.8	−8.0 ± 0.1	0.0	0.0
S/Radcliffe	−8.8 ± 0.1	3.0	2.5	−9.2 ± 0.1	−0.6	−0.6
S/Kempsey	−8.4 ± 0.2	3.5	2.4	−8.7 ± 0.1	−0.36	−0.34
S/Yakima	−9.8 ± 0.2	2.6	1.9	−9.5 ± 0.1	−0.76	−0.74
S/Ypsilanti	−8.7 ± 0.1	3.5	2.1	−11.3 ± 0.2	−1.6	−1.7
S/St. Mande	−14.9 ± 0.1	0.1	−0.7	−6.4 ± 0.1	1.7	−0.1
S/TyGard	−14.3 ± 0.2	0.1	−0.1	−8.0 ± 0.2	0.05	−0.05
S/Abruzzo	−14.6 ± 0.2	0.1	−0.4	−7.2 ± 0.2	0.6	0.2

[a] All values are reported in kcal/mol. See text for notes on propogation of errors. [b] $^0\Delta G_2$ and $^4\Delta G_2$ values are from Pettigrew et al. (1982), Ackers and Smith (1986), Turner (1989), and unpublished results. [c] $^i\delta F_1$ and $^i\delta F_1'$ are calculated for both ligation states using eqs 12, 16, 17.

variants at two states of ligation. The table shows the mutant hybrid system, the location and residue substitution for the particular modification, and the fully deoxygenated and fully oxygenated deviation free energies. Locations within a particular interface or contact region are assigned on the basis of whether a modification site is within 4 Å of said interface or contact region as classified by Sack et al. (1978). The majority of the sites we have examined in this survey are in the $\alpha^1\beta^2$ interface and are known to be on the functional pathway for cooperative ligation (the exceptions being Abruzzo, TyGard, and Zurich, as well as hemoglobin S).

Several patterns are notable in these data. First, there are almost equal numbers of additive and nonadditive hybrids. Those hybrid molecules that exhibit a nonzero deviation free energy we call *nonadditive*. Nonadditivity is evidence for direct long-range coupling (ca. 15–35 Å in these hybrids) between the two symmetric, identical, modification sites. *Additive* hybrids are those with deviation free energies of zero within error. If two sites are additive, their effect on the function of interest is independent. It can be seen in Table I that, for all hybrids studied, the deviation free energy (δ) is either zero or positive with a magnitude of less than 1.35 kcal/mol.

Table II reports the values of the deoxy and oxy dimer to tetramer assembly free energies ($^i\Delta G_2$) determined in this laboratory for the mutant parent hemoglobins studied herein (Pettigrew et al., 1982; Turner, 1989; and unpublished results). The δ and $^i\Delta G_2$ values for each mutant are used via the thermodynamic linkage in Figure 8 and eqs 12, 16, and 17 to calculate the functional perturbation due to the "first" (δF_1) and the "second" ($\delta F_1'$) of the two "identical" structural modifications, and these values are also reported in Table II. A deviation free energy (δ) of zero yields equality of δF_1 and $\delta F_1'$. Inequality of δF_1 and $\delta F_1'$ reflects direct energetic communication between the two sites.

The energetic coupling of any two sites is always defined within the context of the function one is assaying. When one examines the deviation free energies of either deoxygenated hybrids or oxygenated hybrids alone, the context in which dependent sites are communicating is the function of subunit assembly. To address whether two sites demonstrate dependent or independent effects relative to cooperative ligand bind, one must ask whether δ changes with ligation. We define the difference δoxy − δdeoxy as δ^{coop}, or the cooperativity-linked deviation free energy. Values of δ^{coop} for the mutant hybrids studied are listed in Table III. One can see that there are a few definite examples of direct long-range coupling but that most hybrids are additive with respect to cooperativity. Also notable is that the magnitude of the cooperativity-linked deviation free energies (δ^{coop}) corresponding to direct coupling effects is small compared to the individual site perturbation free energies ($\delta\Delta G_c1$ and $\delta\Delta G_c1'$) in any hybrid system.

Table III: Functional Perturbations of the Cooperative Energetics of Asymmetric Mutant Hybrids[a]

mutant hybrid	ΔG_c[b]	δ^{coop}[c]	$\delta\Delta G_c1$[d]	$\delta\Delta G_c1'$[d]
A/S (reference)	6.3 ± 0.2	−0.05 ± 0.15	0.05	−0.05
S/Kariya	1.7 ± 0.2	−0.09 ± 0.16	2.4	2.2
S/Chesapeake	2.1 ± 0.3	0.06 ± 0.36	2.0	2.2
S/Dallas	1.9 ± 0.3	−0.02 ± 0.14	2.2	2.2
S/Tarrant	1.8 ± 0.3	−0.02 ± 0.14	2.5	2.1
S/St. Claude	3.1 ± 0.2	−0.44 ± 0.70	2.0	1.2
S/desArg	1.1 ± 0.2	−0.05 ± 0.20	2.65	2.55
S/Austin	7.5 ± 0.3	0.00 ± 0.64	−0.6	−0.6
S/Athens GA	8.1 ± 0.5	−0.09 ± 0.23	−0.8	−1.0
A/Zurich	6.0 ± 0.2	−0.09 ± 0.22	0.2	0.1
S/thiomethylated	5.8 ± 0.2	−0.17 ± 0.22	0.4	0.1
S/NES	3.0 ± 0.2	−0.01 ± 0.20	1.66	1.64
S/Hotel Dieu	0.2 ± 0.2	−0.25 ± 0.14	3.3	2.8
S/Radcliffe	−0.4 ± 0.2	−0.21 ± 0.14	3.6	3.1
S/Kempsey	−0.3 ± 0.2	−0.53 ± 0.14	3.8	2.8
S/Yakima	0.3 ± 0.2	−0.32 ± 0.14	3.3	2.7
S/Ypsilanti	−2.6 ± 0.2	−0.63 ± 0.16	5.1	3.8
S/St. Mande	8.5 ± 0.2	0.51 ± 0.30	−1.6	−0.6
S/TyGard	6.3 ± 0.3	−0.04 ± 0.23	0.04	−0.04
S/Abruzzo	7.4 ± 0.3	−0.01 ± 0.14	−0.54	−0.56

[a] All values are in kcal/mol. See text (Theory, section III) for notes on propogation of errors. [b] ΔG_c is calculated by using eq 18. [c] δ^{coop} is calculated by using eq 19. [d] $\delta\Delta G_c1$ and $\delta\Delta G_c1'$ are calculated by using eqs 18, 21, and 22.

Table IV shows distribution of the mutant hybrid hemoglobins we have studied into five categories of functional coupling. Taking into account the associated errors on the various δ values, some of the hybrids qualify for more than one category (Tarrant and Austin), while others qualify for subclasses of the major classes. To foster the most useful comparison, we show the least complex pattern distribution in Table IV.

Table IV: Patterns of Functional Coupling Found among Asymmetric Mutant Hybrids[a]

class			
I	$\delta oxy \approx \delta deoxy \approx 0$	$\delta^{coop} = 0$	S,[b] Kariya,[b] Chesapeake,[b] Dallas, Tarrant,[c] Athens GA,[b] Zurich,[b] β93 thiomethylated,[b] TyGard
II	$\delta oxy \approx \delta deoxy \neq 0$	$\delta^{coop} = 0$	desArg, NES, Austin,[d] Abruzzo, St. Claude
III	$\delta oxy \neq \delta deoxy = 0$	$\delta^{coop} \neq 0$	none
IV	$\delta deoxy \neq \delta oxy = 0$	$\delta^{coop} \neq 0$	Hotel Dieu, Radcliffe, Kempsey, Yakima, Ypsilanti
V	$\delta oxy \neq \delta deoxy \neq 0$	$\delta^{coop} \neq 0$	St. Mande

[a] Classifications are based on data in Tables I and III. [b] Borderline cases that actually do show a small amount (≤0.2 kcal/mol) of direct coupling, which is not cooperativity-linked ($\delta^{coop} = 0$). [c] Tarrant may also be classified in group IV. [d] Within error, Austin may also be classified in group I.

In Table IV it can be seen that about half the mutant hybrid hemoglobins studied exhibit little or no direct coupling in either the oxy or deoxy ligation states (class I). Among the other half, there are direct couplings which are cooperativity linked ($\delta^{coop} \neq 0$) and those which are not ($\delta^{coop} = 0$). In other words, hybrids S/desArg, S/NES, and S/Abruzzo are nonadditive by the same amount in both the deoxy and oxy ligation states, whereas all the β99 mutant hybrids as well as S/St.Mande show a significant difference in energetic coupling depending on the ligation state. This appears to be evidence for two different types of direct communication pathways, one of which is linked to cooperative ligation, the other of which is not.

Discussion

Quantitative Cryogenic Isoelectric Focusing. This paper describes results using a technique that we have developed for accurately determining relative assembly free energies of hemoglobins undergoing complex equilibria to form asymmetric hybrids. The new theory and methods of quantitation developed in this work augment the elegant quenching and separation procedures developed by Perrella and associates (Perrella et al., 1978, 1981, 1983; Perrella & Rossi-Bernardi, 1981).

Several lines of evidence have led us to the conclusion that this technique is thermodynamically valid. Simulations of the relationship between initial fractions of parent tetramers and equilibrium fractions (Figure 7) will only agree with experiment if the experiment is an accurate representation of the true equilibrium.

Changing the conditions of the cryogenic quench is an excellent way to assay for systematic perturbation from equilibrium. If particular quench conditions were causing a perturbation of the hybrid equilibrium, one would expect other quench conditions to perturb the equilibrium in other specific ways. Changing the pH and ionic strength of the buffer over wide ranges does not yield significant changes in the deviation free energies obtained (LiCata, 1990).

Eight of the forty hybrids in Table I have been studied previously in our lab by other techniques (Smith, 1985; Ackers & Smith, 1986; Grasberger et al., in preparation). Previous studies from this laboratory on unligated asymmetric hemoglobin hybrids utilized a kinetic technique involving sophisticated analysis of the multiexponential decay observed when one monitors the rate of tetramer dissociation using haptoglobin to trap free dimers (Ackers & Smith, 1986; Smith, 1985). Previous studies on oxygenated hybrid equilibria utilized gel permeation chromatography (Grasberger et al., in preparation). These earlier studies detected mostly additive hybrids within the experimental accuracy of the techniques used. The small nonadditive effects which were observed were difficult to establish as significant. The increased sensitivity to small deviations from additivity which QC-IEF affords has allowed definitive detection of direct long-range pathways of communication within the hemoglobin tetramer. The fact that the magnitudes of these nonadditivities is relatively small is in agreement with these earlier studies. Within calculated error limits, the earlier and present studies agree very well (±<0.1 kcal/mol).

General agreement between the cryogenic IEF technique, gel permeation chromatography, and kinetic studies of hybrid hemoglobins additionally supports the thermodynamic validity of the cryogenic isoelectric focusing results. These methods and theoretical approaches are adaptable to any system where ligand binding, conformational change, or protein polymerization bring about a detectable change in p*I* or electrophoretic mobility.

Functional Coupling across the $\alpha^1\beta^2$ Interface. We observe both direct and indirect functional coupling between symmetric sites in hemoglobin relative to the functions of subunit assembly and cooperativity. It is certainly significant that none of the 40 asymmetric mutant hybrid hemoglobins surveyed herein exhibit a negative value of δoxy or δdeoxy. This indicates that the assembly free energy of the hybrid when it is not additive is always displaced toward lower than additive stability. It is not clear what may be the origin of such an observation. QC-IEF appears to be a valid method for "trapping" and quantitating these hybrid equilibria, and so this observation is indicative of some fundamental aspect of the energetic coupling in hemoglobin. It is possible that there are symmetry-related subunit association processes which when symmetrically perturbed result in less functional damage than when asymmetrically perturbed.

A similar effect is seen when the values of δoxy and δdeoxy are combined into the quantity δ^{coop}: the perturbation to the cooperative free energy by the "first" modification is (within error) always equal to or greater than the effect of the "second" modification. The absence of negative values for δoxy and δdeoxy does not automatically mean that $|\delta\Delta G_c1| \geq |\delta\Delta G_c1'|$. The actual values of δoxy and δdeoxy and ΔG_c for S/St. Mande, along with the curious absence of "class III" hybrids as categorized in Table IV, result in this observation. This may be indicative of a characteristic of functional coupling during cooperative ligation in human hemoglobin, or of a small sample size.

The values of energetic perturbations caused by the "first" ($^i\delta F_1$) and the "second" ($^i\delta F_1'$) of the two "identical" structural modifications are reported in Table II. In either ligation state the difference $^i\delta F_1 - {}^i\delta F_1'$ can be considered a type of anticooperativity of perturbation effects. For example, in the case of deoxy S/St. Claude the "first" modification produces 3.0 kcal/mol of energetic perturbation to dimer–tetramer assembly. The "second" modification's effect is anticooperative by 2.7 kcal/mol, thus introducing only 0.3 kcal/mol additional perturbation energy. Since the sites are structurally identical, this effect cannot be attributed to intrinsic site heterogeneity.

Using Table II, it is interesting to compare the magnitude of the free energy of "anticooperative communication" between two sites ($^i\delta F_1 - {}^i\delta F_1'$) with the magnitude of perturbation to the functional energetics caused by the structural modifications [$(1/2)^i\delta F_{(2)}$]. In about half the hybrids studied we find that the free energy of "anticooperative communication" constitutes a significant portion of the functional perturbation energy introduced by the structural modification. This suggests that

direct coupling plays a fairly significant role in the function of subunit assembly.

In the case of cooperative ligation, direct energetic coupling plays a less significant role (Table III). Most of the sites assayed show independence of effects on the function of cooperativity. Whereas half of all hybrids assayed showed direct coupling in either the oxy or deoxy ligation states, when δ^{coop} is calculated, that percentage decreases due to two effects: (1) the observed nonadditivity in the deoxy and oxy ligation states did not change and therefore is not linked to cooperativity, or (2) propagation of errors obliterates the nonadditivity of δ^{coop}.

The fact that all asymmetric hybrids are within 0.63 kcal/mol of being additive relative to cooperativity while the mean perturbation to cooperativity by a single site alteration $[(1/2)(\delta\Delta G_c1 + \delta\Delta G_c1')]$ can be as great as 4.5 kcal/mol suggests that the major mode of energy transduction across the $\alpha^1\beta^2$ interface does not involve direct long-range couplings but instead consists of an indirect communicative network where symmetric residues on opposite sides of the $\alpha^1\beta^2$ interface are functionally independent of one another, yet both linked to cooperative switching of the molecule. The fact that a structural alteration at any one site on this indirect pathway can eliminate a relatively large fraction of the 6.3 kcal/mol of cooperative free energy available to the molecule suggests that this "indirect pathway" consists of a delicate balance of forces. The exact nature of this indirect energetic pathway could range from a network of discrete triangulation effects where communication between two sites requires propagation through a third site (e.g., the heme) to a global switching process wherein all the interactions involved in generation of a particular function are altered simultaneously and independently as the molecule switches through a series of global states.

Speculation as to the nature of the detailed structural bases resulting in the functional energetics observed using the strategies of "mapping by structure–function perturbation" must be approached cautiously. In Table III we observe that the largest direct coupling effects *among the hemoglobins we have examined* occur at the β99 position and at position β102 (St. Mande). The β99 position is part of a hydrogen bonding contact between the β FG corner and the α C helix within a region of the $\alpha^1\beta^2$ interface known to undergo significant movement (on the order of 6 Å) upon ligation (Baldwin & Chothia, 1979). The two symmetric β FG corner–α C helix contacts are known as the "switch" regions, and there is a hydrogen bond between the β99 position and the α42 position within the switch region that is eliminated upon ligation. The values of δ^{coop} for the alterations at the β99 position indicate that the two switch regions directly communicate during cooperative ligation. These two regions are approximately 20 Å apart in the molecule, so there obviously is no single hydrogen bond or salt bridge responsible for this energetic coupling.

The β99 position is also involved in a hydrogen bond with position α97 which forms part of the contact between the α and β FG corners and which is eliminated upon ligation. Position α40 is also involved in a hydrogen bond that is broken upon oxygenation (with β146). Both positions α97 and α40 appear to exhibit exclusively indirect energetic coupling relative to cooperative ligation. The β102 position (St. Mande) is found to exhibit a large degree of functionally important direct energetic coupling and is found to be part of a hydrogen bond which forms upon ligation between the α and β FG corners (Baldwin & Chothia, 1979). Positions α126 and α127 both form "salt bridges" in the deoxy tetramer with the α141 arginine on the opposite α chain. These bonds are both eliminated upon ligation. These two residues may or may not be involved in cooperativity-linked direct long-range coupling as propagated errors obliterate what seem to be large direct coupling effects. It is interesting to note that while the nonadditivities of hemoglobins Tarrant (α126) and St. Claude (α127) differ dramatically in both the deoxy and oxy ligation states (see Table I), when their cooperativity-linked deviation free energies are calculated, they are seen to be similar in effect.

Whether a particular residue site exhibits exclusively indirect coupling with its symmetric equivalent or both indirect and direct coupling effects does not seem to be correlated in any way with any particular structural events such as large relative movements or the making or breaking of hydrogen bonds during ligation. There is no a priori reason why there should be any such correlation. The finding of direct energetic coupling between two sites tells us nothing about the actual noncovalent or covalent bonds through which the energetic communication occurs. It tells us that such a pathway must exist, but until many more hybrid combinations are examined, and are examined as a function of extrinsic variables such as pH and temperature, we can state only whether or not a pathway exists and describe some of its general characteristics.

The results obtained in this study suggest that there are both independent and nonindependent elements to the energetic communication during cooperative ligation in human hemoglobin. The overall pathway of functional coupling seems to be indirect in nature, wherein the two halves of the regulatory interface act nearly independently. Within this indirect context, however, there is some network, or set of networks, of direct long-range communication within the tetramer which operates at a lower energetic magnitude. We view the theoretical approaches and experimental studies herein as prototypes for understanding aspects of how regulatory information is energetically communicated within proteins in general.

Registry No. O_2, 7782-44-7.

References

Ackers, G. K., & Halvorson, H. R. (1974) *Proc. Natl. Acad. Sci. U.S.A. 71*, 4312–4316.

Ackers, G. K., & Smith, F. R. (1985) *Annu. Rev. Biochem. 54*, 597–629.

Ackers, G. K., & Smith, F. R. (1986) *Biophys. J. 49*, 155–165.

Anbari, M., Adachi, K., Ip, C. Y., & Asakura, T. (1985) *J. Biol. Chem. 260*, 15522–15525.

Baldwin, J., & Chothia, C. (1979) *J. Mol. Biol. 129*, 175–220.

Bevington, P. R. (1969) *Data Reduction and Error Analysis for the Physical Sciences*, McGraw-Hill, New York.

Bunn, H. F. (1981) *Methods Enzymol. 76*, 126–133.

Bunn, H. F., & McDonough, M. (1974) *Biochemistry 13*, 988–993.

Ip, C. Y., & Asakura, T. (1984) *Anal. Biochem. 139*, 427–431.

Ip, C. Y., & Asakura, T. (1986) *Anal. Biochem. 156*, 348–353.

Ip, S. H. C., Johnson, M. L., & Ackers, G. K. (1976) *Biochemistry 15*, 654–660.

LiCata, V. J. (1990) Ph.D. Dissertation, The Johns Hopkins University.

Mills, F. C., Johnson, M. L., & Ackers, G. K. (1976) *Biochemistry 15*, 5350–5362.

Park, C. M. (1970) *J. Biol. Chem. 245*, 5390–5394.

Park, C. M. (1973) *Ann. N.Y. Acad. Sci. 209*, 237–257.

Penefsky, H. S. (1977) *J. Biol. Chem. 252*, 2891–2899.

Perrella, M., & Rossi-Bernardi, L. (1981) *Methods Enzymol. 76*, 133–143.

Perrella, M., Heyda, A., Mosca, A., & Rossi-Bernardi, L. (1978) *Anal. Biochem. 88*, 212-224.
Perrella, M., Cremonesi, L., Benazzi, L., & Rossi-Bernardi, L. (1981) *J. Biol. Chem. 256*, 11098-11103.
Perrella, M., Benazzi, L., Cremonesi, L., Vesely, S., Viggiano, G., & Berger, R. L. (1983) *J. Biochem. Biophys. Methods 7*, 187-197.
Pettigrew, D. W., Romeo, P. H., Tsapis, A., Thillet, J., Smith, M. L., Turner, B. W., & Ackers, G. K. (1982) *Proc. Natl. Acad. Sci. U.S.A. 79*, 1849-1853.
Sack, J., Andrew, L., Magnus, K., Hanson, J., Rubin, J., & Love, W. (1978) *Hemoglobin 2*, 153-169.
Schroeder, W. A., & Huisman, T. H. J. (1980) *The Chromatography of Hemoglobin*, Marcel Dekker, New York.
Smith, F. R. (1985) Ph.D. Dissertation, The Johns Hopkins University.
Smith, F. R., & Ackers, G. K. (1985) *Proc. Natl. Acad. Sci. U.S.A. 82*, 5347-5351.
Turner, B. W., Pettigrew, D. W., & Ackers, G. K. (1981) *Methods Enzymol. 76*, 596-628.
Turner, G. J. (1989) Ph.D. Dissertation, The Johns Hopkins University.
Williams, R. C., & Tsay, K. (1973) *Anal. Biochem. 54*, 137-145.

Alteration of Sperm Whale Myoglobin Heme Axial Ligation by Site-Directed Mutagenesis†

Karen D. Egeberg,‡ Barry A. Springer,‡ Susan A. Martinis, and Stephen G. Sligar*
Departments of Biochemistry and Chemistry, University of Illinois, Urbana, Illinois 61801
Dimitrios Morikis§ and Paul M. Champion*
Department of Physics, Northeastern University, Boston, Massachusetts 02115
Received November 15, 1989; Revised Manuscript Received July 16, 1990

ABSTRACT: Three mutant proteins of sperm whale myoglobin (Mb) that exhibit altered axial ligations were constructed by site-directed mutagenesis of a synthetic gene for sperm whale myoglobin. Substitution of distal pocket residues, histidine E7 and valine E11, with tyrosine and glutamic acid generated His(E7)Tyr Mb and Val(E11)Glu Mb. The normal axial ligand residue, histidine F8, was also replaced with tyrosine, resulting in His(F8)Tyr Mb. These proteins are analogous in their substitutions to the naturally occurring hemoglobin M mutants (HbM). Tyrosine coordination to the ferric heme iron of His(E7)Tyr Mb and His(F8)Tyr Mb is suggested by optical absorption and EPR spectra and is verified by similarities to resonance Raman spectral bands assigned for iron–tyrosine proteins. His(E7)Tyr Mb is high-spin, six-coordinate with the ferric heme iron coordinated to the distal tyrosine and the proximal histidine, resembling Hb M Saskatoon [His(βE7)Tyr], while the ferrous iron of this Mb mutant is high-spin, five-coordinate with ligation provided by the proximal histidine. His(F8)Tyr Mb is high-spin, five-coordinate in both the oxidized and reduced states, with the ferric heme iron liganded to the proximal tyrosine, resembling Hb M Iwate [His(αF8)Tyr] and Hb M Hyde Park [His(βF8)Tyr]. Val(E11)Glu Mb is high-spin, six-coordinate with the ferric heme iron liganded to the F8 histidine. Glutamate coordination to the ferric iron of this mutant is strongly suggested by the optical and EPR spectral features, which are consistent with those observed for Hb M Milwaukee [Val(βE11)Glu]. The ferrous iron of Val(E11)Glu Mb exhibits a five-coordinate structure with the F8 histidine–iron bond intact. The results presented here demonstrate the power of site-directed mutagenesis as a tool for altering the electronic structure of metal centers and aiding in the assignment of complicated vibrational spectra.

Heme proteins are ubiquitous, assuming varied roles in biochemistry. Typically, they are classified on the basis of their ligation to the iron center. Four of the six heme iron coordinate positions are occupied by protoporphyrin IX pyrrole nitrogens with one or both of the two remaining coordinate positions occupied by the protein moiety. Six-coordinate electron-transfer proteins include bis-imidazole-ligated *b*-type cytochromes and the methionine–histidine coordination of *c*-type cytochromes. Heme proteins with an open coordination site include the oxygen storage and transport proteins (myoglobin and hemoglobin) and peroxidases with histidine ligation, catalases with tyrosine ligation, and cytochromes P-450 and chloroperoxidase with cysteine as the fifth axial ligand. The iron–imidazole bond in myoglobin (Mb) and hemoglobin (Hb) and its effect on the iron–porphyrin out of plane displacement (Srajer et al., 1988) are thought to have a major role in the mechanisms which control ligand affinity and the transition of the R to T state in Hb [Perutz (1970, 1987) and references cited therein].

The construction of a synthetic gene for sperm whale Mb and the resultant high-level expression of this gene as heme-containing protein in *Escherichia coli* (Springer & Sligar, 1987) have enabled us to genetically engineer sperm whale Mb by in vitro mutagenesis techniques. Substitution of the proximal histidine (F8) with a tyrosine, His(F8)Tyr,[1] the distal

† This work was supported by NIH GM33775 and NIH GM31756 (S.G.S.) and NIH AM35090 and NSF DMB8716382 (P.M.C.).
* To whom correspondence should be addressed.
‡ Present address: Department of Chemistry, University of California, Berkeley, CA 94720.
§ Present address: Department of Molecular Biology, Research Institute of Scripps Clinic, La Jolla, CA 92037.

0006-2960/90/0429-9783$02.50/0